

RESEARCH ARTICLE

Open Access



Spectral information to get beyond color in the analysis of water-soluble varnish degradation

M. Martínez Domingo^{1*} , E. Valero¹, R. Huertas¹, M. Durbán², T. Espejo² and R. Blanc³

Abstract

Spectral images were captured of paper samples varnished with two water-soluble materials: gum arabic and egg white. The samples were submitted to degradation processes that partially or totally eliminated the varnish from the substrate (water immersion and ageing). The spectral information was used to obtain average color data and to characterize the spatial and color inhomogeneity across pixels, showing that the pixel spectral data are critical for an accurate characterization of the degradation process of the varnishes. Since the varnishes typically become yellower with ageing, this study introduces two novel and simple-to-compute yellowness indices based on the spectral information, which are validated against a standard colorimetric index (ASTM-E313 2015). The potential uses of spectral information are demonstrated with several pieces of a real antique map sample by comparing the spectral information measured before and after cleaning the sample. To sum up, the main contributions of this study are the characterization of the spatial homogeneity through pixel-based spectral and color information and the proposal of spectral-based yellowing indices for two critical applications (ageing process follow-up and effect of cleaning), as demonstrated with synthetic and historical samples of varnished paper respectively.

Keywords: Yellowness index, Spectral reflectance, Spectral imaging, Cultural heritage

Introduction

Spectral imaging is an emerging tool in analysis in the field of conservation and restoration of Cultural Heritage (CH) [1, 2]. Some of the most relevant applications found are the identification of pigments and materials used in the original artworks [3, 4], the characterization of the preservation state using spectral ranges beyond the visible [5] and the visualization of hidden layers or “pentimenti” using the infrared range [6]. However, few studies have focused on the use of spectral imaging on the ageing process of the materials commonly used in artworks or ancient texts [7, 8].

Besides characterizing the degradation of pigments or colorants, it is essential for the preservation of artworks to be able to quantitatively characterize the state

of ageing of the varnishes applied, bearing in mind that different varnishes show different behavior with ageing [9, 10].

The processes involved in the degradation of varnishes have been widely studied by means of either analytic techniques, such as IR, UV spectroscopy or gas/mass chromatography [11, 12]; or colorimetric methods [13]. However, varnish degradation on a graphic support—whether paper or parchment—is less known.

Throughout history, graphic works of different kinds have been varnished, either for aesthetic reasons or for protection. Applying a varnish increases the brightness and saturation of colors, and also provides a different artistic effect to the artwork. Nevertheless, varnishes are mainly applied for their protective qualities, as they prevent the mechanical, environmental or biological deterioration of the work. To this end, many materials have been used, mainly natural resins, but also protein-based materials and natural gums [14], which are the materials we discuss in this study.

*Correspondence: martinezdm@ugr.es

¹ Optics Department, Faculty of Sciences, University of Granada, Granada, Spain

Full list of author information is available at the end of the article

Egg white and gum arabic have been used since the Middle Ages on all kinds of graphic arts. Up until the 16th century it was common to protect miniatures in order to increase their brightness and protect them from mechanical deterioration caused by their continuous use [15] with the same materials used as paint binders or the adhesives of gold foils [16]. Over the subsequent centuries, the use of these materials diversified. The painter Edgar Degas (1834–1917) applied different materials, gum arabic among them, as a binding agent in thin layers, in order to both protect his pastel paintings and create different effects [17]. In the nineteenth century, egg white and gum arabic were applied as intermediate varnishes before applying a resin-based varnish [16]. This technique, typical of easel painting, aims to create an isolating coat that prevents the resin from penetrating the paper and the varnish solvents dissolving the binding agents [18]. In the twentieth century the above-mentioned materials were used as a final varnish; for instance, the German painter George Grosz (1893–1959) protected his water-color paintings with a final coat of egg white [19].

These works of art reflect a symbiosis between paper and varnish, as the features of one will directly affect the behavior of the other and can even reduce or accelerate the degradation process [20, 21], and there are marked differences in behavior across different varnishes. Thus, it is essential to know such features as behavior and alteration processes in order to choose the correct intervention criteria in restoration processes aimed at their elimination, maintenance or possible replacement. Amongst of all of them, color is a major element in a varnish, as the possible changes in it will substantially alter the aspect of the underlying work, modifying its appearance and/or making it difficult to read and appreciate.

The aim of this study is to show convincingly that spectral imaging information can add value to relatively simple color analysis and other invasive procedures (such as pH determination) which are usually carried out in the CH field to characterize the degradation processes of varnishes.

Materials and methods

Sample preparation and size of selected areas

The varnishes studied in this paper are soluble in water. Gum arabic (GA) and egg white (EW) samples were prepared following traditional recipes [15] and applied according to standard procedures using an airbrush device. Two layers of undiluted varnish were applied (1:6 solution in water for GA). For simplicity, in the following, unvarnished and varnished samples are referred to under the acronyms 0% and 100% respectively. The substrate material used for all the samples was

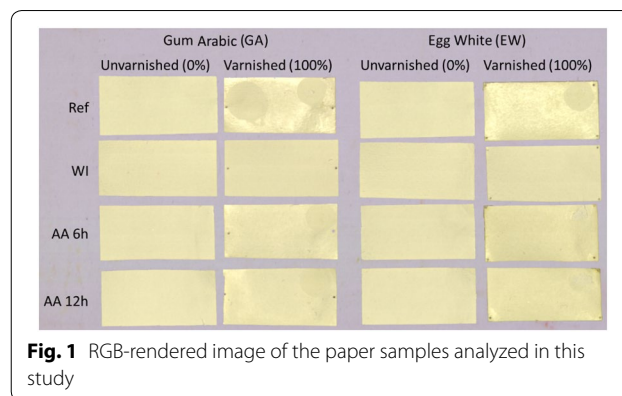


Fig. 1 RGB-rendered image of the paper samples analyzed in this study

100% cotton Somerset paper (acid-free), prepared in 50×25 mm pieces.

For the analysis, in the captured images, an area of 122×122 pixels was selected around the sample center, equivalent to 19×19 mm.

Spectral imaging device and data acquisition

Samples were captured with a Resonon PikaL VIS–NIR line-scan camera [22] in 150 bands from 380 to 1000 nm in 4 nm steps. The data were cropped to the 400 to 950 nm range due to low signal to noise ratio (SNR) in the extreme wavelengths of the spectrum, and interpolated with a regular step of 5 nm for convenience of use, resulting in 111 bands (from 400 to 950 nm in 5 nm steps). The illumination used for the capture was a halogen lamp provided by the manufacturers of the device for lighting the linear stage in which the samples were placed (see Fig. 1 for a false-*RGB* rendered example image). Spectral imagers commonly respond to the light signal coming from the imaged sample, which is the product of the spectral power distribution of the illumination and the spectral reflectance of the sample. In order to retrieve only the information from the sample, the information from the illumination must be discounted using a flat field procedure [23]. For such purpose, a Teflon white reference tile also provided by the manufacturers was used. Spatial illumination inhomogeneities and dark signal were corrected by the device internal calibration procedure.

Sample degradation procedures and substrate homogeneity

Two degradation processes were studied: water Immersion (WI) and accelerated ageing in an ageing chamber (AA). The WI process was selected to test if our analysis technique was able to detect the effect of the varnish disappearance as a consequence of its solubility in water. For the WI, the samples were submerged for 180 min,

according to norm UNE-EN-ISO 2812-2:2007 [24]. For the AA, a SolarBox 3000eRH chamber was used, with the settings at 80 °C, 65% of relative humidity, UV radiation of 550 w/m², for 6 h and 12 h, according to norm ISO 5630-3:1996 [25]. The ageing times were not extremely long, because the aim was to be able to characterize subtle color and material variations.

Comparisons were made with unvarnished reference samples (different pieces of paper for each process and varnish condition). The homogeneity of the substrate reference samples was assessed computing the color and spectral metrics described in the next sub-sections in a measured batch of 30 122 × 122 pixel areas.

Color characterization

For each pixel spectral reflectance, CIELAB L^* , a^* , b^* coordinates were calculated under equienergy illumination. L^* , a^* , b^* coordinates were also calculated for the average spectral reflectance of the measurement area, mimicking what a standard spectrophotometer would provide, although for this instrument the measurement of spectral reflectance would be performed with different illumination/observation settings. The standard deviation values were also calculated for the L^* , a^* , b^* distributions, as a means to characterize the spatial inhomogeneity of the samples.

Color differences were calculated using the standard CIEDE2000, ΔE_{00} , color difference formulae [26]. For the analysis of the CIEDE2000 color difference values, the threshold for noticeable color differences is considered to be 1 CIEDE2000 unit, higher than usual tolerances for industrial materials [27].

For the study of yellowing in the AA degradation experiment, the ASTM standard E313 Yellowing index was calculated from tristimulus values under illuminant C [28], following the equation:

$$CI = 100 \frac{(C_x X - C_z Z)}{Y}$$

with X , Y and Z the tristimulus values of the sample under illuminant C, and $C_x = 1.2764$, $C_z = 1.0592$ for the CIE-1931 Standard Observer.

Spectral characterization

The mean spectral reflectance was calculated for each measured area, by averaging the 122 × 122 spectral reflectances captured by the line-scan device. The standard deviation for each wavelength was also calculated as a way to characterize the spatial non-homogeneity of the samples, and the average standard deviation across the different wavelengths was also calculated.

For the study of yellowing in the AA degradation experiment, two novel spectral yellowness indices were introduced as follows:

- Spectral Yellowness Index 1 (SYI_1 , wide-band): this is based on the ratio of the sum below the reflectance curve in two wide spectral ranges, which are characterized by a typically low reflectance (400 to 470 nm) or high reflectance (550 to 950 nm) in yellow samples that present the typical roughly step-shaped spectral reflectance curve. The two initial bands for computing the ratio were selected by varying the starting wavelength (between 400 and 465 nm for the lower band, and between 550 nm and 945 nm for the upper band) and computing the correlation of the index obtained with the CI index. The lower band covered from the initial wavelength up to 470 nm, and the upper band from the initial wavelength in the upper range up to 950 nm. The two initial wavelengths selected by this procedure were 400 and 550 nm, and the SYI_1 was accordingly defined as:

$$SYI_1 = \frac{\sum_{\lambda=550}^{\lambda=950} R(\lambda)}{\sum_{\lambda=400}^{\lambda=465} R(\lambda)}$$

- Spectral Yellowness Index 2 (SYI_2 , narrow-band): this index is also based on the ratio of two integrated spectral bands, but the bands are much narrower than for the SYI_1 (10 nm bandwidth). The optimal two bands have been selected by maximizing the correlation with the CI index from all possible combinations of band ratios between 400 and 940 nm. The best correlation was obtained for the bands 440 nm and 610 nm. The SYI_2 index would be more sensitive to local changes in the spectral reflectance curves and at the same time, it would be more sensitive to variations in a particular wavelength range, which could be of interest for certain applications.

$$SYI_2 = \frac{\sum_{\lambda=610}^{\lambda=620} R(\lambda)}{\sum_{\lambda=440}^{\lambda=450} R(\lambda)}$$

As spectral difference metrics, the Root Mean Square Error and the Goodness-of-Fit-Coefficient have been used [29].

Results

The results will be presented in this section for each of the two experiments performed: WI and AA, in each sub-section, the analysis will start with the information which would be provided by the standard instruments

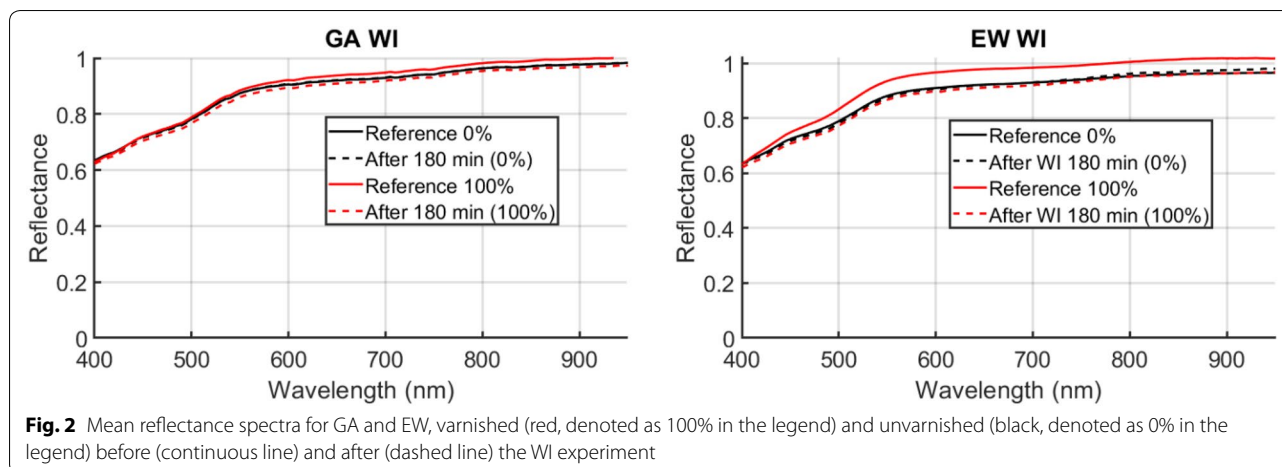


Table 1 RMSE, GFC and CIEDE2000 values of the average spectral reflectance curves (calculated over the visible range) for the WI and AA experiments

	GA			EW		
	RMSE	GFC	CIEDE2000	RMSE	GFC	CIEDE2000
WI						
0% vs 100%	0.0134	0.9999	0.7	0.0470	0.9999	1.8
0% vs 0% after WI	0.0020	1.0000	0.2	0.0050	1.0000	0.3
100% vs 100% after WI	0.0240	1.0000	0.7	0.0586	0.9999	2.0
0% vs 100% after WI	0.0121	1.0000	0.4	0.0097	1.0000	0.3
AA						
0% vs 0% after AA 6 h	0.0041	1.0000	0.1	0.0067	1.0000	0.3
100% vs 100% after AA 6 h	0.0114	1.0000	0.3	0.0708	1.0000	1.9
0% vs 0% after AA 12 h	0.0196	1.0000	0.5	0.0055	1.0000	0.2
100% vs 100% after AA 12 h	0.0043	1.0000	0.3	0.0625	1.0000	1.7

(spectrophotometer and then colorimeter). Then, the added value of the analysis of the spatial homogeneity of the samples in the spectral domain will be described. The color information (both from averaged results and spatial homogeneity characterization) will also be analyzed. Moreover, the yellowness indices values and their validation against the standard colorimetric index E313 (only in the AA experiment) are calculated. Finally, the results obtained using the real vintage map sample will be presented and discussed.

Homogeneity of the substrate

The homogeneity of the substrate reference samples was assessed by measuring a batch of 30 122 × 122 pixel areas. The mean reflectance values of these areas were used to compute the color and spectral metrics. The average and maximum (minimum for GFC) values obtained were: 0.2674 and 0.7658 respectively for ΔE_{00} ; 1.0000 and 0.99996 for GFC; and 0.0072 and 0.0257 for RMSE.

These values are well within the acceptable quality range. The substrate color and spectral homogeneity was then satisfactory.

WI experiment

First, the data of average spectral reflectances of the samples were analyzed for the different experimental conditions tested. Figure 2 shows the spectral reflectance curves obtained by averaging all the reflectance curves pixel-by-pixel.

It can be observed how the varnished reference curves present some values slightly over 1, especially for the EW samples. This is likely to be due to the presence of specular reflections in these samples, as can be also noted in the rendered picture of Fig. 1. This factor contributes to the spatial inhomogeneity of the varnished samples, which will be analyzed later.

In Table 1, the spectral difference metrics results calculated from the average spectra are shown for the

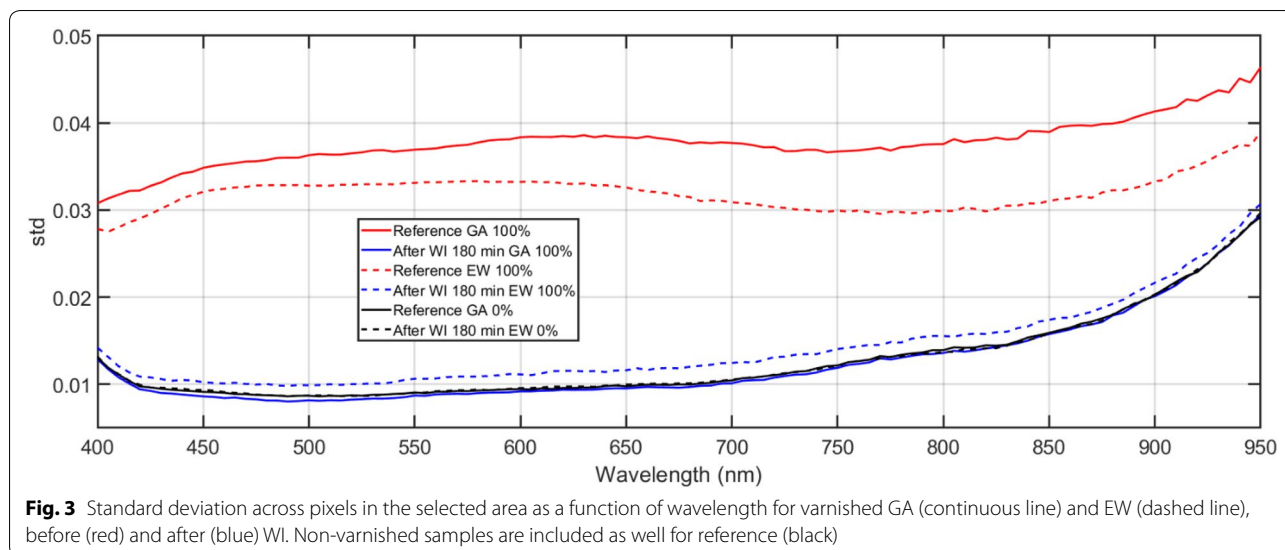


Fig. 3 Standard deviation across pixels in the selected area as a function of wavelength for varnished GA (continuous line) and EW (dashed line), before (red) and after (blue) WI. Non-varnished samples are included as well for reference (black)

following sample pairs: unvarnished vs varnished (0% vs 100%), unvarnished before vs unvarnished after WI (0% vs 0% after WI), varnished vs varnished after WI (100% vs 0% after WI), and unvarnished vs varnished after WI (0% vs 100% after WI). As an additional safety check, the two unvarnished reference samples (0% in the figure) for GA and EW were compared, yielding a ΔE_{00} difference of 0.3015, and RMSE of 0.0048 in the VIS range, with $GFC=1$ ($cGFC=1-GFC=1122e-05$), well within the range of typical color and spectral differences found for the substrate [mean ΔE_{00} of 0.2674 (std=0.1666), mean RMSE of 0.0072 (std=0.0051), and mean GFC of 1 (std=8e-6)], see "Homogeneity of the substrate" section.

After the WI process, the mean spectra of the varnished samples are remarkably more similar to the unvarnished reference and WI samples. This could be explained by considering the hypothesis that the WI process has eliminated the varnish from the paper substrate, since both varnishes are soluble in water: the spectral differences would be within the usual tolerance for measurement errors (GFC above 0.999 and RMSE below 2.5% [29]), implying that there would not be any detectable changes in the average reflectance after WI. The effect of the varnishing (0% vs 100% sample pair) is more noticeable in the mean spectra of the EW samples than for the GA samples.

In the comparisons listed in the first column of Table 1, we can observe how, there would not be any noticeable difference for the GA samples. For the EW samples, however, there would be clear color changes due to varnishing (1.8 CIEDE2000 units), and WI for varnished samples (2.0 units). Visually, the color rendered samples shown

in Fig. 1 also support the assumption that (even for the EW varnished samples) the color differences are barely perceptible in terms of mean color after WI, but the disappearance of the layers of varnish is visibly noticed in terms of spatial homogeneity of the sample, as is shown below.

Since there are hardly any noticeable differences according to the previous analysis (except for the EW varnished sample), additional analyses were carried out which arose from the idea that maybe the WI could even slightly alter the spatial homogeneity of the paper samples. The variations in spatial homogeneity are totally ignored in the conventional color difference metric values analysis shown above. Standard deviation across the pixels and as a function of wavelength was then introduced as a metric to roughly quantify this texture effect. The advantage of spectral information, provided by multi-spectral measurements, is that the dependence of spatial homogeneity with the wavelength can be studied, something that would not be possible when using area-based spectral measurement devices or an imaging colorimeter (such as a calibrated color camera). As an example, in Fig. 3 the standard deviation as a function of wavelength is shown for the different varnished samples tested in the WI experiment.

The curves shown in Fig. 3 suggest that the behavior of the standard deviation is not uniform across wavelengths within the visible range. There is a trend to increase the standard deviation for the medium-to-long wavelength range in the varnished samples and then decrease it around 700 nm, which is not present in the samples after WI and which must be then attributed to the effect of the varnish deposition, which is not even for

Table 2 Average STD values across wavelengths for WI experiment, for unvarnished (0%) and varnished (100%) GA and EW samples

	Average STD over wavelength 0%	Average STD over wavelength 100%
WI		
Reference GA	0.0126	0.0377
GA After WI 180 min	0.0128	0.0123
Reference EW	0.0126	0.0319
EW After WI 180 min	0.0126	0.0141
AA		
Reference GA	0.0126	0.0377
GA after 6 h	0.0125	0.0177
GA after 12 h	0.0119	0.0169
Reference EW	0.0126	0.0319
EW after 6 h	0.0121	0.0184
EW after 12 h	0.0117	0.0147

all the wavelengths. There is also a clear trend towards higher inhomogeneity for the NIR wavelengths in both varnished and unvarnished samples. This trend could be explained in terms of the lower signal-to-noise ratio (SNR) for the NIR bands, due to the decrease in sensor responsivity that the increase of energy emitted in the NIR wavelengths by the light source is not able to compensate. The difference in standard deviation due to the WI process is also lower in this range, which may also support the hypothesis that the lower SNR could contribute to making this range poorer in terms of discriminative ability.

The average standard deviation values across wavelength (see Table 2) are very similar for varnished and unvarnished samples after WI, while they were much higher for unvarnished samples before WI. For the GA varnished samples, even if the spectral difference metrics were not able to detect any variations as a result of the WI process, the analysis based on the spatial homogeneity of the samples is clearly able to detect the change induced by the immersion in water as an increase in spatial homogeneity (decrease in the standard deviation values). For the EW samples, similar behavior to the GA samples is found, with a relatively lower decrease of the average standard deviation for the EW varnished sample after WI, and no decrease for the unvarnished sample.

If we compare the STD plots in Fig. 3 between GA (continuous line) and EW (dashed line) varnished samples, there are some minor differences as well, which may be due to the different effects of the varnish deposit, since the airbrush application is not perfectly reproducible and the two varnishes have different chemical and physical

properties. Finally, the undeniable similarity between the unvarnished and the varnished samples after WI support the hypothesis previously suggested by the analysis of the mean reflectance values, regarding the likely disappearance of the varnish layers after the WI process.

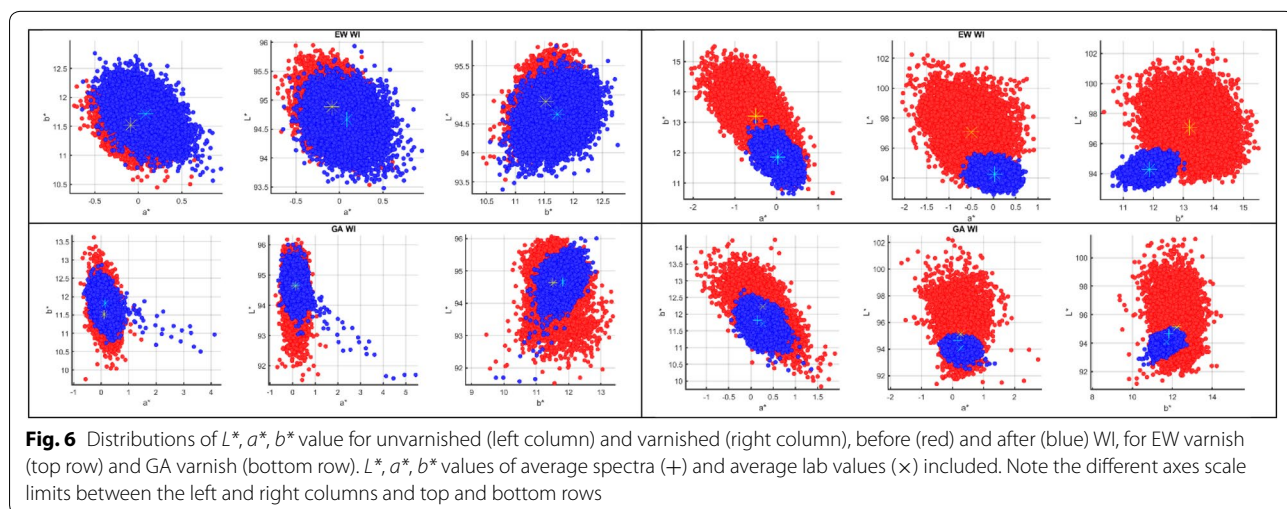
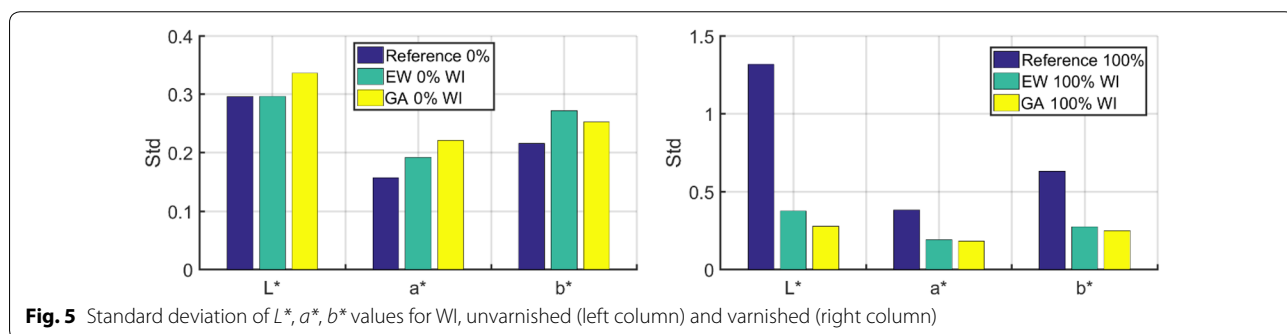
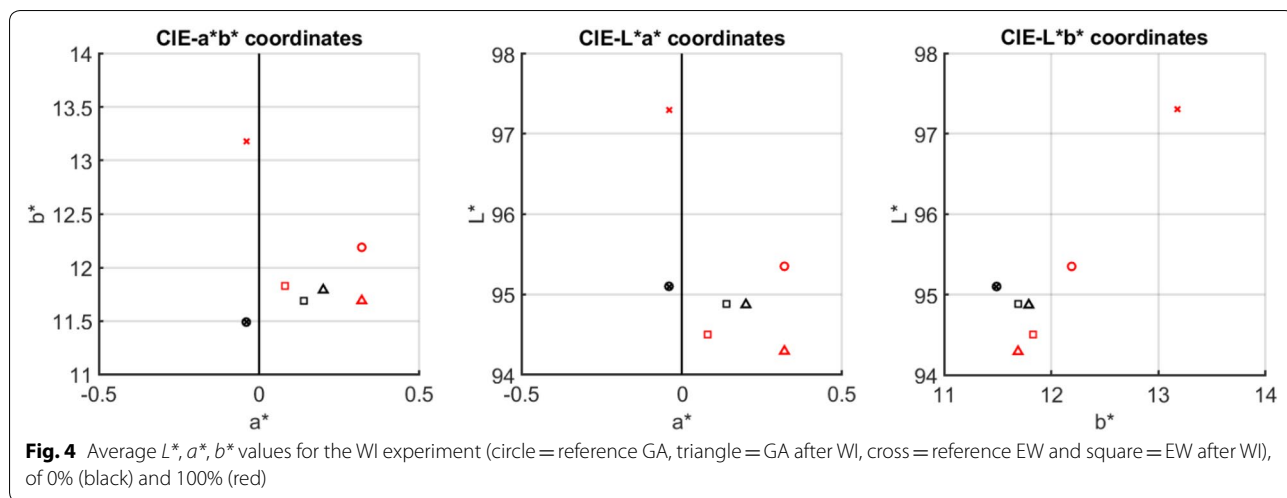
These results show that using the standard deviation analysis, we can quantitatively characterize even differences in the varnish cover of the sample that are not detected by analyzing the mean reflectance spectra, nor by other chemical standard procedures such as pH measurement (the GA and EW samples remained neutral both before and after WI, with a maximum pH variation of 0.2 and pH values ranging from 7.1 to 7.6).

The standard deviation values obtained using the batch of 30 Somerset paper reference samples ranged from 0.0162 to 0.0210, with a mean of 0.0174 (std=0.0011). These results show that basically the WI samples have the same spatial homogeneity as the typical substrate samples, whilst the varnished samples clearly have lower spatial homogeneity.

Now the color characterization results are analyzed. Regarding the average L^* , a^* , b^* values, in general, we found that the average L^* , a^* , b^* values calculated using the whole distribution of L^* , a^* , b^* values for each sample are very similar to those calculated using the average spectral reflectance spectra. This is as expected, although the transformation from spectra to L^* , a^* , b^* involves non-linearities, and therefore the means are not necessarily preserved.

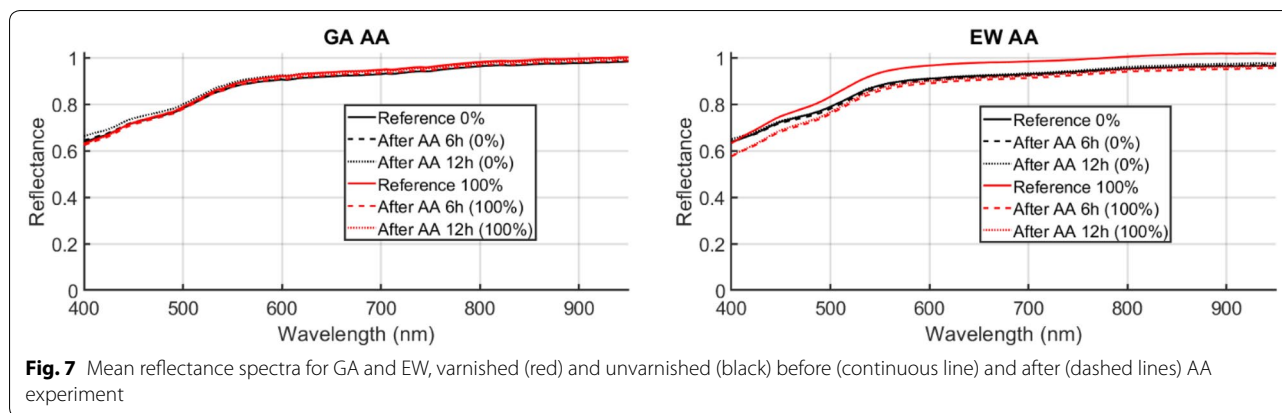
For the GA samples (see Fig. 4), the effect of varnishing produced a small increase in L^* , a^* and b^* values, reflected by the relatively small CIEDE2000 color difference value for the comparison between 0 and 100% GA samples (shown in Table 1). The effect of WI for the unvarnished sample is very slight, whilst for the varnished sample it is a bit higher, with L^* and b^* presenting lower values. For the EW samples, the variation in L^* , a^* , b^* values is higher (in agreement with the higher values of color differences shown in Table 1). This suggests that there is likely to be a perceptible change in color due to the varnishing (with increasing L^* and b^* coordinates), and after WI the L^* , a^* , b^* values of both unvarnished and varnished samples are much more similar than before WI, and both L^* and b^* decrease, in agreement with the trend found for the GA samples.

Using the individual pixel L^* , a^* , b^* distributions instead of average values, the STD values are calculated and presented in Fig. 5. These results are mostly in agreement with the findings previously reported when analyzing the spectral STD values. The effect of varnishing and WI for the GA samples, that are barely noticeable using the average L^* , a^* , b^* values and CIEDE2000 color difference, becomes much clearer when looking at the trends



presented by the spatial homogeneity of the sample. As expected, using the L^* , a^* , b^* values to compute this spatial inhomogeneity has less potential than using the full spectrum, because less information is extracted from each sample.

The L^* , a^* , b^* value distribution plots for the different conditions are presented in Fig. 6. This visualization is convenient for showing the increased spatial homogeneity of the varnished samples after WI, whilst the unvarnished samples remain mostly stationary. The



average L^* , a^* , b^* values are also shown in Fig. 6, which serves to illustrate the different capabilities of an analysis based just on conventional area-based measurements (one point per sample) and the analysis based on the full information provided by a spectral imaging device (or an imaging colorimeter in this case).

Figure 6 shows that the L^* , a^* , b^* distributions are also sensitive in a noticeable and quantifiable way to the color and texture changes taking place in the samples, with a clear gamut shape change for the WI varnished samples towards a shrinking of the L^* , a^* , b^* clouds after WI, as expected given the increase in spatial homogeneity that presumably results from the dilution of the varnish layer. Having the possibility of analyzing these distributions is an asset over having only the mean L^* , a^* , b^* values and color differences to detect these changes, especially if they are barely noticeable as in the case of the GA varnish.

AA experiment

The changes in mean spectra are in general slight for the GA and EW samples, as shown in Fig. 7. Nevertheless, the effect of ageing on the varnished samples is much more noticeable for the EW varnished than for the GA varnished samples. The varnished samples tend towards lower reflectance values, whilst the unvarnished papers tend towards higher reflectance values as they ages. This shows that the varnish is probably darkening as it ages, especially in the initial stage of 6 h; however, the spectral difference metrics values shown in Table 1 suggest that these differences would hardly be noticeable for the GA varnish, and they would be noticeable in scale (RMSE values) for the EW samples, which is also in agreement with the curves shown in Fig. 7.

For the GA samples, the CIEDE2000 data in Table 1 show that the effect of the varnishing is barely noticeable, and that the effect of ageing could not be visually detected. For the EW varnished samples, the CIEDE2000

values show that both the effect of varnishing and the effect of ageing on the varnished samples would be noticeable (color differences above 1.0 CIEDE2000 units).

Regarding the spatial homogeneity results, presented in Table 2, the average spectral standard deviation values are shown for the GA (first three rows) and EW (rows four to six) for the reference and aged varnished and unvarnished samples.

The spatial homogeneity tends to increase both for unvarnished and varnished samples (as shown by decreasing average standard deviation values as the ageing time increases), although it increases more in relative terms for the varnished samples. The change from 6 to 12 h ageing for the varnished samples is not as high as the change between the reference samples and 6 h ageing.

The standard deviation plots shown in Fig. 8, confirm these findings. The difference between 6 and 12 h ageing is slight in terms of STD across the wavelengths, especially for the unvarnished samples. The changes in spatial homogeneity are also much smaller for the NIR range compared with the visible range. The trend towards higher standard deviation values for longer wavelengths is also present. The spatial homogeneity proves to be a more sensitive parameter for determining changes in the samples induced in the GA varnished samples, which were not noticeable using the mean spectral reflectance data, nor the pH determination (with a maximum variation of 0.2 in pH for the aged GA samples). The curves in Fig. 8 suggest that ageing is slower in terms of spatial homogeneity increase for the EW varnish than for the GA varnish.

Regarding the colorimetric data analysis, Fig. 9 shows the L^* , a^* , b^* values calculated using the average spectral reflectance spectra. According to this, for the GA samples the variations in L^* reflect those of the mean reflectance curves: for the unvarnished sample, L^* does only increase slightly after 12 h's ageing, whilst a^* fluctuates slightly and b^* is mostly unchanged with a slight trend towards

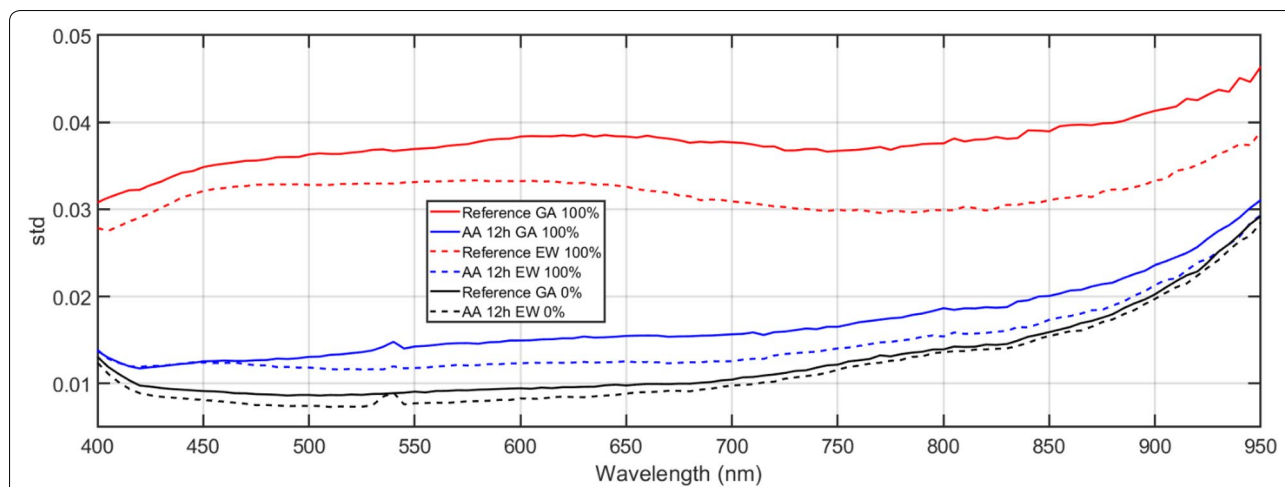


Fig. 8 Standard deviation across pixels in the selected area as a function of wavelength for varnished GA (continuous line) and EW (dashed line), before (red) and after (blue) AA 12 h. Non-varnished samples are included as well for reference (black)

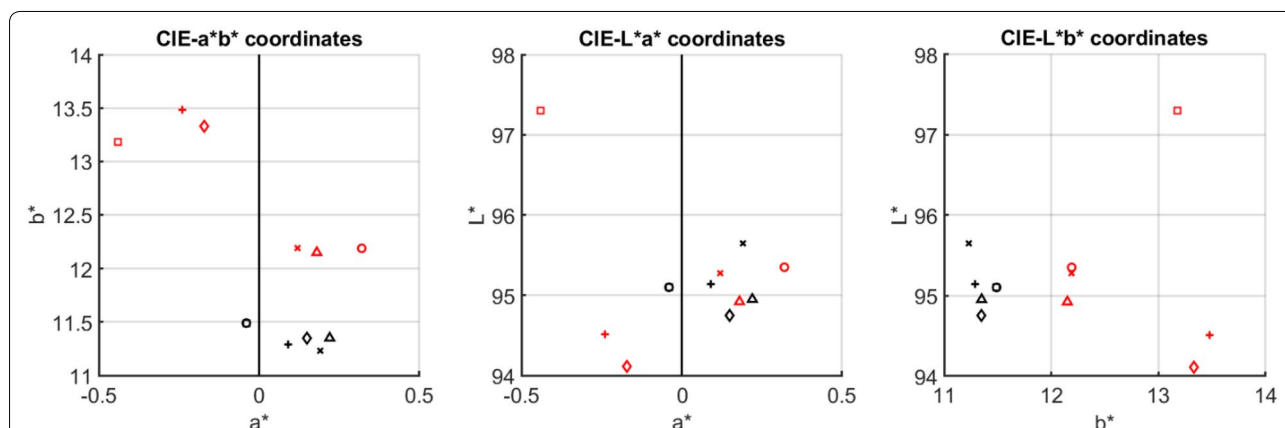


Fig. 9 Average L^* , a^* , b^* values for the AA experiment (circle = reference GA, triangle = GA after 6 h, cross = GA after 12 h, square = reference EW, diamond = EW after 6 h, and plus = EW after 12 h), of 0% (black) and 100% (red)

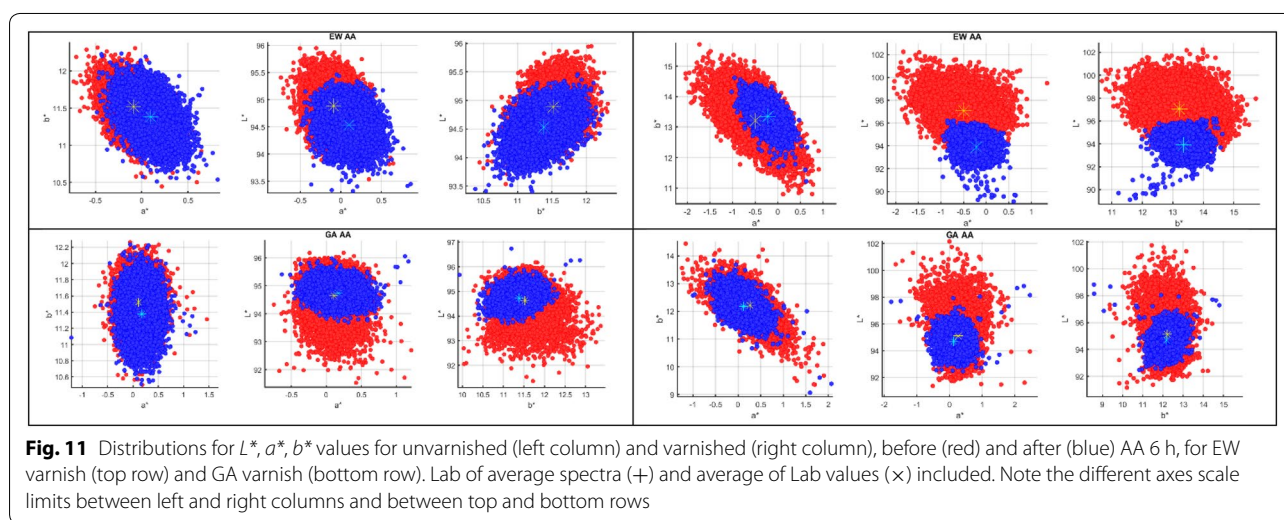
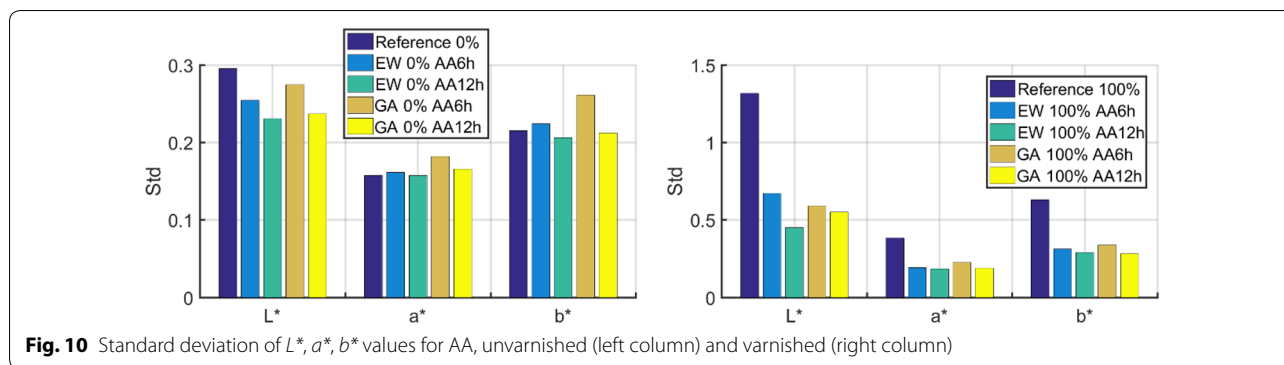
decreasing with the ageing time. For the varnished AG samples, L^* decreases slightly initially for 6 h’s ageing, and approximates the initial value for 12 h’s ageing, whilst a^* shows a tendency to decrease and b^* remains stationary. Overall (and considering the color difference metric as well), we could doubt the significance of the fluctuations found.

For unvarnished EW samples there are very similar fluctuations in L^* , a^* and b^* values as those found for the GA unvarnished samples (this is logical since unvarnished samples are constituted by the substrate paper). Considering the effect of ageing on the EW varnished sample, L^* and a^* become lower (with some fluctuations for the 12 h sample, which is more similar to the varnished reference, as shown in the reflectance curves);

for the b^* coordinate, there is a consistent trend towards increasing b^* values, which could be described as “yellowing”.

Regarding the standard deviation values in L^* , a^* , b^* values, the same trends commented for the WI experiment are found. In general, the standard deviation data show the same trends already commented for the L^* , a^* , b^* values of the mean spectra section as well. There is (as noticed when analyzing the mean spectral STD data) a tendency towards a more marked decrease in inhomogeneity for the varnished samples as they age (see Fig. 10).

We also show the L^* , a^* , b^* distributions for the AA experiment in Fig. 11. Here again, as in the case of WI experiment, we can see a noticeable difference in homogeneity after the ageing, especially for the varnished



samples, even if the mean color of the distributions does not change very much in the $a^* - b^*$ plane or for the GA varnished samples.

For the unvarnished samples, the effect of ageing is slightly more noticeable than the effect of water immersion (as seen in Fig. 6).

Characterization of yellowing for the AA experiment

To further analyze the results of the AA experiment, two novel spectral yellowness indices and the well-known ASTM E313 colorimetric yellowness [28] index were calculated, as described in "Materials and methods" section. The reason to focus on characterizing yellowness is that this is the expected effect caused by ageing, especially for the varnished samples; it is the price to pay for the varnish protection of the substrate. An increase in yellowness could in principle be characterized by hue values closer to the 90° axis, and an increase in chroma possibly also linked to a decrease in the lightness of the samples. Nevertheless, after having calculated the h_{ab} and C^*_{ab} values for all the samples, the trends found are not clear enough, very likely

due to the subtle effects analyzed especially for the GA samples and the fact that the Somerset paper already had a yellow tinge to begin with. So, the hypothesis is then that reverting to the use of the yellowness indices will prove to be more useful for the detection of color changes linked to the ageing process.

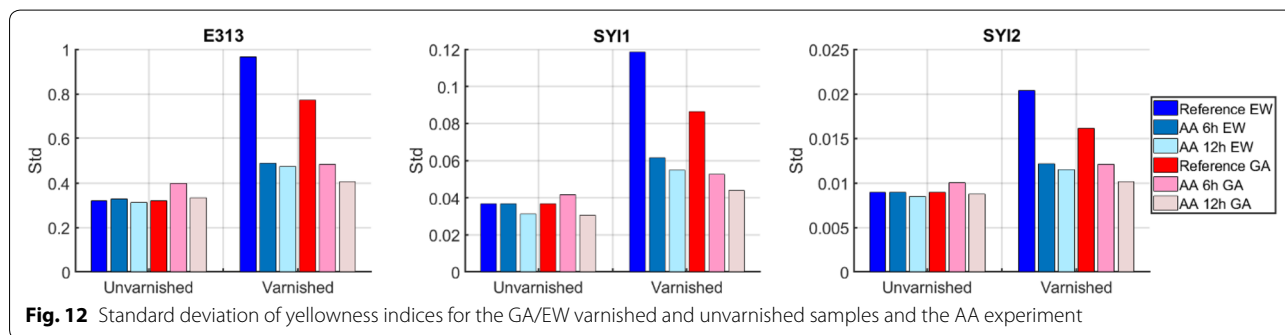
The spectral yellowness indices offer the following advantages over the E313 index:

- They are independent of the illumination, but they can easily be extended to predict the yellowness of the samples under different illuminations by redefining the spectral indices in terms of the color signal instead of the reflectance.
- They do not have any parameters to be tuned with a set of reference samples, as was done for the E313 index.

Their main disadvantage seems to be that they are less sensitive, thus the relative variation between conditions is lower in the samples analyzed for the SYI indices than for the E313 index.

Table 3 Average yellowness indices

	Unvarnished 0%			Varnished 100%		
	E313	SY11	SY12	E313	SY11	SY12
Reference GA	2020	729	128	2157	752	1301
GA after 6 h	2019	733	1276	2146	749	1298
GA after 12 h	1986	728	1269	2142	748	1296
Reference EW	2020	729	1277	2226	753	1316
EW after 6 h	2018	730	1275	2328	770	1332
EW after 12 h	1996	727	1271	2338	772	1333



In Table 3, the average values of the three yellowness indices are shown for the GA and EW samples.

The average yellowness indices' results for the GA varnish indicate consistent findings with those obtained analyzing the color of the samples, although we are now able to be specific in targeting color changes towards yellow. The effect of varnishing with GA is a slight increase in yellowness, whilst the effect of ageing is consistent for both unvarnished and varnished samples, i.e. a slight reduction in yellowness.

The findings for the EW unvarnished samples are consistent with those found for the GA samples, i.e. mostly stationary values with slight fluctuations. For the varnished samples, however, the trend towards yellowing is very strongly confirmed by using these indices, with consistent findings for the three indices used and a more noticeable increase in yellowness for the varnished samples.

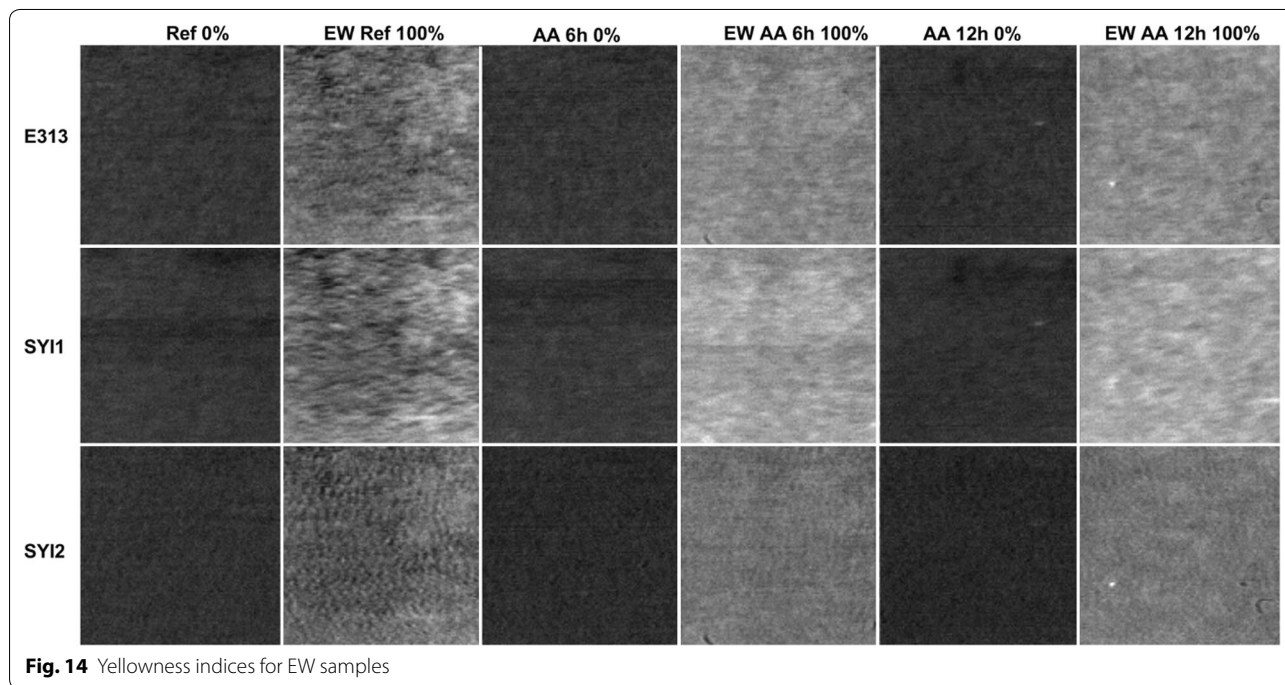
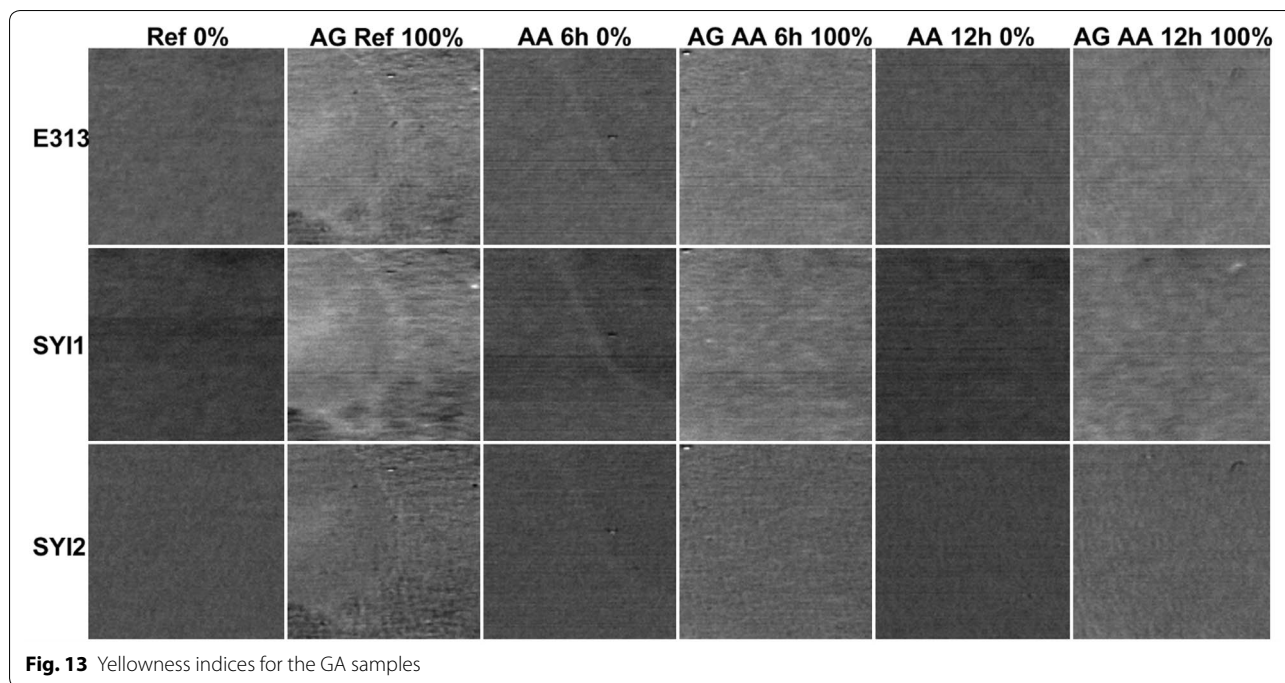
Since the yellowness indices are calculated on a pixel-by-pixel basis, the standard deviation data can also be analyzed. They are graphically represented in Fig. 12. The trends found are in agreement with those described in the previous sections: higher uniformity (lower standard deviation values) for the aged samples and for the unvarnished samples.

The three indices offer consistent values, which will be further explored later on. However, the relative variation of the E313 is higher.

Figures 13 and 14 show a gray-scale image representation of the three indices (pixel-by-pixel corresponding with the imaged samples), which offers the opportunity to explore the spatial variations of the yellowing process (even if they are slight, as in this case). It is interesting to notice how the spatial inhomogeneity of the substrate is also reflected in the yellowness index, as well as the effect of the dropping in the varnished reference sample, which is more yellow around the borders and within the confines of the dropping (possibly reflecting a higher amount of varnish deposited locally). The different sections of the figure are normalized so as to also represent the relative variations in yellowness indices in all conditions, so the unvarnished samples are noticeable darker (less yellow) than the varnished samples, and the aged samples spatially more homogeneous and slightly more yellow than the reference varnished samples.

The consistent results obtained for the three metrics analyzed lead to the following conclusions:

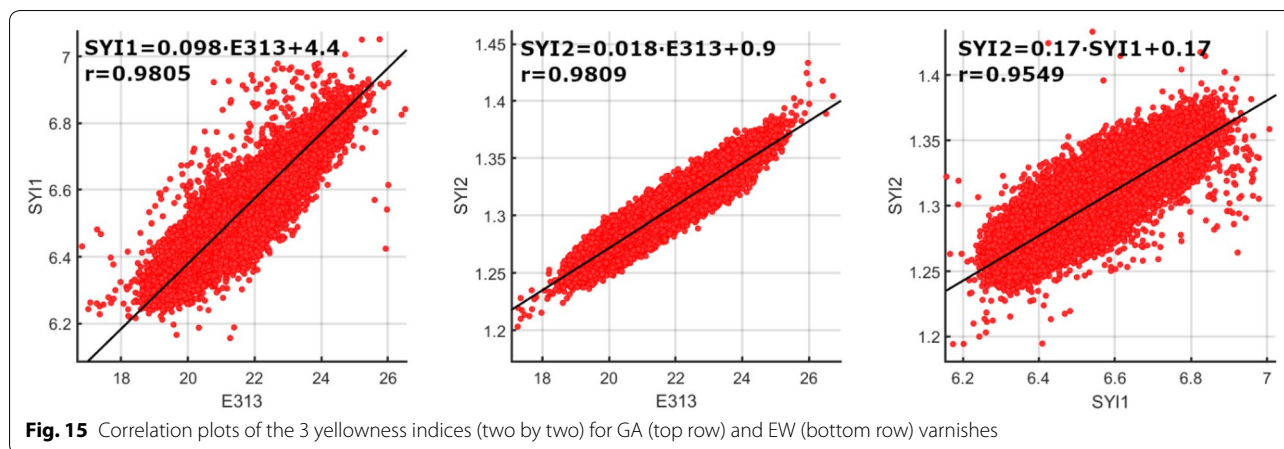
- The unvarnished samples tend not to be altered (except a slight variation in spatial homogeneity) by the ageing process. This might be due to not overly prolonged times in the ageing chamber.
- The GA varnished samples show a slight trend towards decreasing yellowness, whilst the EW varnished samples yellow perceptibly. This indicates



that GA is colorimetrically more stable to ageing. This is partly supported by [30], where the main components of plant gums are shown to be stable to thermal oxidation, though in our case, also

humidity and UV radiation were applied to the samples.

The two proposed spectral yellowness indices have not yet been properly validated with a controlled sample set. Nevertheless, given the high number of pixels analyzed in



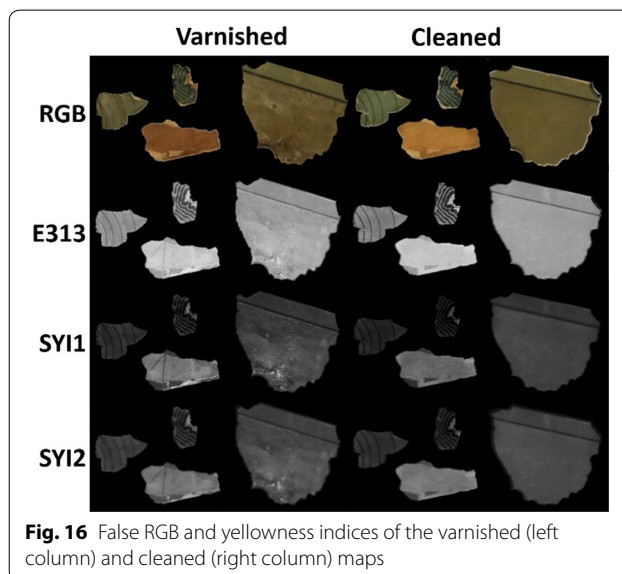
this study, a correlation analysis can be performed to analyze consistency of each pair of indices values, by pooling together the unvarnished and varnished sample data. The results of this analysis are described in terms of correlation coefficient values (*r*) and linear fit plots (see Fig. 15). There is in general some degree of correlation between the three pairs of indices defined, with the highest values corresponding to E313 and SYI-2, and the lowest to the two spectral yellowness indices.

Vintage map sample analysis

An illustration of the capabilities of the analysis methods presented in the previous section using real samples of historical value is presented in this section.

The map collection from which the samples have been extracted consists of forty-six physical-political maps with different contents, dated between 1875 and 1982, belonging to the Granada University Archive. They are wide-format documents, printed on paper, varnished, laid on to cloth and placed on wood strips. In general terms, the cellulose and textile supports were weak, with marked wrinkles and deformations on the paper due to the differential movements between paper and fabric. There were also numerous tears and missing parts, damp patches and blanching on the protective coat as a consequence of direct dampness. The work started in 2016 on six wide-format maps, of which four are still being treated. They were chosen because of their high degree of deterioration and the urgent need for restoration to prevent any further damage. A working protocol was established, which included historical, material and technical research, an analysis of the conservation status, an establishment of the diagnosis and the application of a treatment.

Four small pieces which were already detached from two of these vintage maps as a result of their ageing were selected for analysis. The four map pieces were captured



in their original aged state using our hyper-spectral line scanner, and then again after a cleaning was performed which is supposed to partially or totally eliminate the aged varnish layer. The cleaning treatment was carried out in two stages: first by means of capillarity, stippling the map surface with absorbent material impregnated with organic solvents until the maximum amount of varnish was removed. The second stage involved letting a continuous flow of water go through the same absorbing material to achieve, by means of conduction, the combined cleaning of the paper and the fabric that made up the support of the maps.

A color rendered image of the pieces is presented in Fig. 16 (top row), before and after the cleaning procedure. It can be observed how the map pieces include different pigments and the original paper substrate can also be seen in some pieces around the borders.



Fig. 17 False RGB image of maps with three different pigments highlighted and mean reflectance spectra of each pigment

Table 4 Yellowness indices and L^* , a^* , b^* statistics for maps. Mean values (and STD)

	E313	SY11	SYI2	L^*	a^*	b^*
All before	50.12 (16.93)	16.55 (5.50)	2.11 (0.52)	65.57 (5.81)	4.67 (5.29)	19.96 (5.65)
All after	45.70 (19.78)	15.31 (4.70)	2.03 (0.57)	66.59 (6.48)	2.32 (5.46)	20.69 (8.18)

Using the spectral reflectance image, it would be possible to analyze each pigment separately by isolating the areas of the maps that have similar reflectance curves (see Fig. 17). This could not be done with an area-based device due to the small size of the pigmented zones. However, it is maybe more relevant to perform a global analysis and see what are the effects of the cleaning and assumed varnish disappearance from the samples. To this end, the three yellowness indices and their standard deviation values have been calculated (see Table 4). Some interesting findings appear from these data:

- First, the three yellowness indices are able to correctly predict that the varnished samples (map pieces before the cleaning) are more yellow than the cleaned samples.
- Second, the SY11 index is able to correctly predict the increase in spatial homogeneity of the cleaned samples over the original ones (as reflected by the lower standard deviation values). But this is not so for the E313 and SYI2 indices; this may be attributed to an increase in the contrast of the cleaned samples noticeable in the E313 and SYI2 images, which compensates for the effect of increasing homogeneity of the uniform areas within the map. In other words, the lines after the cleaning produce more spatial variation of yellowness than before the cleaning, and this compensates for the effect of increasing homogeneity after the cleaning procedure in the areas that mostly have one pigment deposited.

The L^* , a^* , b^* distributions have also been analyzed for these real samples (see Table 4, containing average and standard deviation data). The most noticeable effects in the color of the sample after the cleaning are an increase

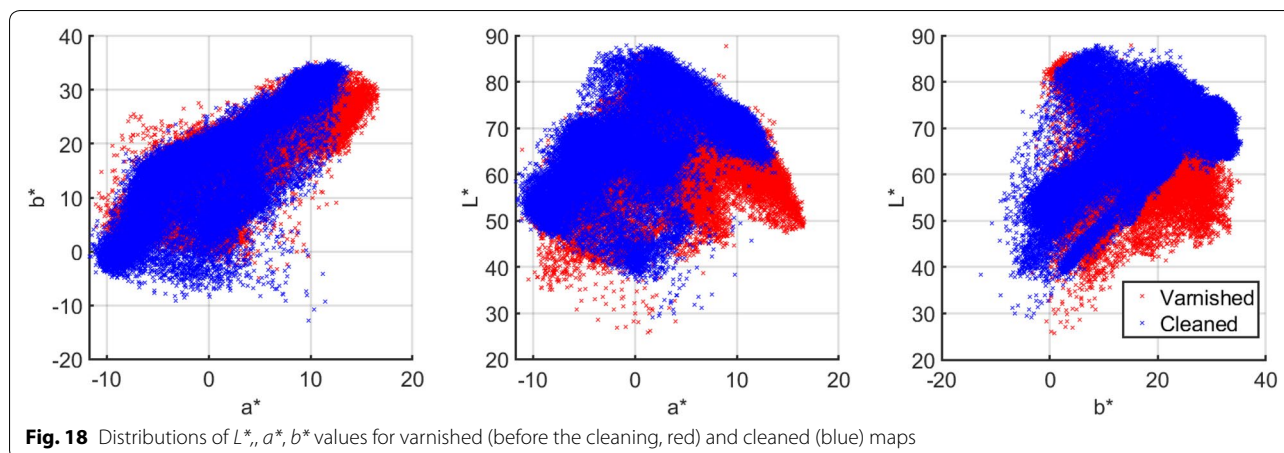
in lightness (L^*) and a decrease in the a^* values, which make the samples on average to have a little less chroma. The average effect on the b^* coordinate is a very slight increase, which makes the results of the yellowness indices much more reliable than just looking at the color coordinates. The average hue angle before the cleaning is 76.83° , and after the cleaning it is 83.60° , which would be contrary to the usual assumed behavior of the hue angle increasing when the samples are more yellow. This angle variation is nevertheless due more to the influence of the decrease in a^* values than to the increase in b^* values after the cleaning. So, the samples behavior could be better described, according to the $a^* - b^*$ values, as “slightly less reddish” after the cleaning.

The standard deviation values are similar in the two conditions according to Table 4, also with a trend to be higher for the cleaned samples, in agreement with the findings reported before with the E313 yellowing index (which is based on color values instead of spectral information).

Finally, in Fig. 18 the L^* , a^* , b^* plots are presented for the map samples before (red) and after the cleaning (blue). In the figure, it can be appreciated how the behavior of the samples is not uniform. For instance: the samples with higher b^* values decrease the a^* value in a higher amount than the samples with lower b^* values. Or the samples with higher a^* and b^* value (the more saturated samples) also tend to increase lightness in a higher amount after the cleaning.

Conclusions and future work

In this study, a complete framework for the spectral information-based analysis of varnished degradation processes is presented. Two varnish degradation processes



which are relevant for water-soluble varnishes have been chosen: WI and AA. The analysis carried out is based on the potential use of a spectral imager as a capturing device, and our results show that it is much more powerful than conventional color analysis for these particular two degradation processes.

Measurements were carried out of both prepared samples and a real example of a varnished map (late nineteenth century) which had aged naturally and been submitted to a cleaning process which eliminated the varnish partially as part of its restoration procedure (carried out as a part of the activities included in the Research grant MAT2014-58659-P. from the Spanish Ministry of Education). In addition, we propose spectral-based yellowing indices that are able to characterize the progression of ageing of varnished samples and the effect of the cleaning performed during the restoration process, as demonstrated with synthetic and historical samples of varnished paper respectively.

In particular, the spatial homogeneity characterization shows good potential for detecting changes in the spectral and color distribution across the different locations within a particular sample, changes that (at least, for the GA varnish) are not noticeable using area-based devices such as a conventional spectrophotometer.

All the data presented show consistent trends which support the hypothesis of the varnish being eliminated almost completely by the WI process, as can be expected. Regarding the AA, even if the ageing times were not very long, the proposed analytical methodology has been able to detect not only changes in color, but also in spatial homogeneity and the color gamut of the samples due to ageing. Moreover, two novel spectral yellowing indices are introduced, of which the one based on narrow spectral bands was found to be better

correlated to the standard yellowness index E313, and to offer slightly more consistent results in the study of the degradation processes. The indices offer the advantage of being tunable to adapt to tackling different spectral changes due to ageing and other degradation procedures, and of being independent of the illumination used to capture the samples.

When real vintage samples are analyzed, the results of the presented method are consistent with the hypothesis that the samples are less yellowish after the varnished layer has been eliminated by cleaning. Analysis of the color distributions shows that the color variations found are different for different colors of the map, which cannot be deduced from the conventional area-based color analysis due to the small size of some pigmented areas.

For future studies it would be interesting to test the applicability of the method for analyzing different varnishes and with longer ageing times. It would also be interesting to use machine learning techniques to test for the feasibility of the automatic classification between varnished and unvarnished of vintage map samples. Finally, assessing the effects of ageing for different areas of the same map and being able to see potential variations due to different preservation conditions would complement the results we have presented.

Acknowledgements

The authors thank the Spanish Ministry of Economy and Competitiveness, the Spanish State Agency of Research and the European Union.

Authors' contributions

MMD: state of the art research, spectral image capture, processing an analysis. EV: spectral image processing and results data analysis. RH: color and spectral data analysis. MD: state of the art research, samples preparation and experimental set up. TE: experimental set up, samples preparation. RB: chemical control of samples. Samples degradation. All authors read and approved the final manuscript.

Funding

Spanish Ministry of Economy and Competitiveness, under research Grant DPI2015-64571-R. Spanish State Agency of Research (AEI) and the Ministry for Economy, Industry and Competitiveness (MIMECO) by means of the Grant Number FIS2017-89258-P with European Union FEDER (European Regional Development Funds) support.

Availability of data and materials

Hyperspectral image data is composed of heavy files. All data recorded in this study can be freely shared upon request.

Competing interests

The authors declare that they have no competing interests.

Author details

¹ Optics Department, Faculty of Sciences, University of Granada, Granada, Spain. ² Painting Department, Faculty of Fine Arts, University of Granada, Granada, Spain. ³ Analytical Chemistry Department, Faculty of Sciences, University of Granada, Granada, Spain.

Received: 14 August 2019 Accepted: 30 September 2019

Published online: 07 October 2019

References

- Cosentino A. Multispectral imaging and the art expert. *Spectrosc Eur*. 2015;27(2):6–9.
- Alvarez-Martin A, Janssens K. Protecting and stimulating effect on the degradation of eosin lakes. Part 1: lead white and cobalt blue. *Microchem J*. 2018;141:51–63.
- Grabowski B, Masarczyk W, Glomb P, Mendys A. Automatic pigment identification from hyperspectral data. *J Cult Herit*. 2018;31:1–12.
- Deborah H, George S, Hardeberg JY. Spectral-divergence based pigment discrimination and mapping: a case study on *The Scream* (1893) by Edvard Munch. *J Am Inst Conserv*. 2019;58:1–18.
- Pottier F, Michelin A, Kwimang S, Andraud C, Goubard F, Lavédrine B. Macroscopic reflectance spectral imaging to reveal multiple and complementary types of information for the non-invasive study of an entire polychromatic manuscript. *J Cult Herit*. 2019;35:1–15.
- Delaney JK, Trumpy G, Didier M, Ricciardi P, Dooley KA. A high sensitivity, low noise and high spatial resolution multi-band infrared reflectography camera for the study of paintings and works on paper. *Herit Sci*. 2017;5(1):32.
- Berns RS, et al. Rejuvenating the appearance of Seurat's *a Sunday on La Grande Jatte—1884* using color and imaging science techniques—a simulation. In: ICOM Committee for conservation preprints: 14th triennial meeting The Hague 2005; 2004.
- Marengo E, Manfredi M, Zerbinati O, Robotti E, Mazzucco E, Gosetti F, Shor P. Technique based on LED multispectral imaging and multivariate analysis for monitoring the conservation state of the dead sea scrolls. *Anal Chem*. 2011;83(17):6609–18.
- Scalalone D, Lazzari M, Chiantore O. Ageing behaviour and pyrolytic characterisation of diterpenic resins used as art materials: colophony and Venice turpentine. *J Anal Appl Pyrol*. 2002;64(2):345–61.
- Azémard C, Vieillescazes C, Ménager M. Effect of photodegradation on the identification of natural varnishes by FT-IR spectroscopy. *Microchem J*. 2014;112:137–49.
- Dietemann P, Higgitt C, Kálin M. Aging and yellowing of triterpenoid resin varnishes—influence of aging conditions and resin composition. *J Cult Herit*. 2009;10:30–40.
- De la Rie ER. Photochemical and thermal degradation of films of dammar resin. *Stud Conserv*. 1988;33:53–70.
- Ciofini D, Striova J, Camaiti M, Siano S. Photo-oxidative kinetics of solvent and oil-based terpenoid varnishes. *Polym Degrad Stab*. 2016;123:47–61.
- Mills J, White R. *Organic chemistry of museum objects*. London: Routledge; 2012.
- Kroustalis S. Binding media in medieval manuscript illumination: a source research. *Revista de História da Arte*. 2011;1:113–25.
- Thompson DV. *The materials and techniques of medieval painting*. Nueva York: Dover; 1956.
- Fletcher S, Santis PD. Degas: the search for his technique continues. *Burling Mag*. 1989;131(1033):256–65.
- Tingry PF. *The painter and varnisher's guide*. Londres: Sherwood, Neely and Jones; 1816.
- Capua R. *Materials and techniques of George Grosz: American water-colors*. 2006.
- Petukhova T. Removal of varnish from paper artifacts. *Book Pap Group Annu*. 1992;11:136–40.
- Colbourne J, Singer B. The removal of natural resin varnished from hand-coloured oil printed media. In: Engel P, editor. *Research in book and paper conservation in Europe: a state of the art*. Viena: Verlag Berger Horn; 2009. p. 51–70.
- W1. <https://resonon.com/pika-l-camera>.
- Martínez MÁ, Valero EM, Nieves JL, Blanc R, Manzano E, Vilchez JL. Multi-focus HDR VIS/NIR hyperspectral imaging and its application to works of art. *Opt Express*. 2019;27(8):11323–38.
- ISO 1: International Organization for Standardization (ISO). *Paints and varnishes—determination of resistance to liquids—Part 2: water immersion method*. UNE-EN ISO 2812-2:2007.
- ISO 1: International Organization for Standardization (ISO). *Paper and board—accelerated ageing—Part 3: moist heat treatment at 80 degrees C and 65% relative humidity*. UNE-EN ISO 5630-3:1996.
- Luo MR, Cui G, Rigg B. The development of the CIE 2000 colour-difference formula: CIEDE2000. *Color research & application: endorsed by Inter-Society Color Council, The Colour Group (Great Britain), Canadian Society for Color, Color Science Association of Japan, Dutch Society for the Study of Color, The Swedish Colour Centre Foundation, Colour Society of Australia, Centre Français de la Couleur*. 2001;26(5):340–50.
- Luo MR, Minchew C, Kenyon P, Cui G. Verification of CIEDE2000 using industrial data. In: *Proceedings of interim meeting of the international color association, AIC 2004 color and paints*, pp. 97–102.
- ASTM E. E313-05 Standard practice for calculating yellowness and whiteness indices from instrumentally measured color coordinates. *Paint-tests for chemical, physical, and optical properties; appearance*; 2005.
- Nieves JL, Valero EM, Hernández-Andrés J, Romero J. Recovering fluorescent spectra with an RGB digital camera and color filters using different matrix factorizations. *Appl Opt*. 2007;46(19):4144–54.
- Brambilla C, Riedo C, Baraldi A, Nevin MC, Gamberini C, D'Andrea O, Chiantore S, Goidanich L Toniolo. Characterization of fresh and aged natural ingredients used in historical ointments by molecular spectroscopic techniques: IR, Raman and fluorescence. *Anal Bioanal Chem*. 2011;401(6):1827.

Publisher's Note

Springer Nature remains neutral with regard to jurisdictional claims in published maps and institutional affiliations.